

## **General Disclaimer**

### **One or more of the Following Statements may affect this Document**

- This document has been reproduced from the best copy furnished by the organizational source. It is being released in the interest of making available as much information as possible.
- This document may contain data, which exceeds the sheet parameters. It was furnished in this condition by the organizational source and is the best copy available.
- This document may contain tone-on-tone or color graphs, charts and/or pictures, which have been reproduced in black and white.
- This document is paginated as submitted by the original source.
- Portions of this document are not fully legible due to the historical nature of some of the material. However, it is the best reproduction available from the original submission.

**NASA Technical Memorandum 79033**

**(NASA-TM-79033) DYNAMIC MECHANICAL ANALYSIS  
OF FIBER REINFORCED COMPOSITES (NASA) 20 p  
HC A02/MF A01 CSCL 11D**

**N79-15157**

**Unclas**

**G3/24**

**42881**

**DYNAMIC MECHANICAL ANALYSIS  
OF FIBER REINFORCED COMPOSITES**

**Katherine E. Reed  
Lewis Research Center  
Cleveland, Ohio**



**TECHNICAL PAPER to be presented at the  
Thirty-fourth Annual Conference of Reinforced Plastics/Composites  
Institute of the Society of the Plastics Industry Inc.  
New Orleans, Louisiana, January 29 - February 2, 1979**

## INTRODUCTION

Dynamic mechanical properties are important factors to consider in the design and application of composite material structures. Young's modulus and internal damping are two such properties and are measures of the stiffness and energy dissipation ability of a substance. Damping, though not well-understood, is a sensitive probe of a wide variety of molecular motions, relaxation processes, transitions, structural homogeneities and morphologies, all of which affect a material's mechanical behavior. In addition, it reduces vibrations and prevents excessive amplitude build-up at resonance frequencies by dissipating energy as heat.

In the region of the glass transition of an amorphous polymer, the modulus undergoes relaxation and the damping curve goes through a maximum. Both phenomena are associated with loosening of the polymer structure to allow segmental and other molecular group motions. The glass transition temperature ( $T_g$ ) of a fiber-reinforced composite is actually the temperature at which changes in thermodynamic properties of the matrix occur since commonly used fiber reinforcements such as carbon and glass fibers do not exhibit such behavior in that temperature region. It has been shown that the presence of a particulate filler increases the  $T_g$  by an amount proportional to the concentration of filler and that the width of the transition region is broadened by increasing filler concentration (ref. 1).

Dynamic mechanical methods have been applied to study the effects of molecular orientation in many polymers including nylon, acrylonitrile-butadiene-styrene, polyethylene terephthalate, and polypropylene (refs. 2-5). Dynamic mechanical studies of reinforced polymers have been concerned primarily with particulate filled thermoplastic matrices. However, the dynamic mechanical behavior of continuous fiber reinforced thermosets has not been extensively studied.

The purpose of this study was to investigate the off-axis resonant frequency and damping characteristics of unidirectional E-glass/epoxy composites. The techniques of mechanical spectroscopy and thermal analysis (differential scanning calorimetry and thermomechanical analysis) were utilized to characterize the dynamic mechanical and thermal properties of the composites.

## EXPERIMENTAL

### Materials

An epoxy/glass system was used in this study whose resin formulation consisted of a diglycidyl ether of bisphenol-A (DER 332), a reactive diluent (RD-2), and a mixed aromatic amine curing agent (Tonox 6040). The fiber was an E-glass continuous filament roving with an epoxy compatible silane finish.

The prepreg material was made by drum winding the E-glass roving at 5 strands per 2.54 cm to a width of 14.9 cm. Two widths of fiber were wound on the drum and heat treated with an infrared lamp to drive off moisture. The resin mixture was formulated as 100gm epoxy: 20gm diluent: 22.8gm amine hardener and was applied to the fiber. The windings were covered and staged at room temperature for 24 hours. They were then cut from the drum in 30 cm lengths and stored at  $-18^{\circ}\text{C}$  in polyethylene bags.

The laminates were prepared in a 15 cm x 30 cm matched metal die and cured at  $82^{\circ}\text{C}$  and 100 psig pressure for 5 hours and were not post-cured unless otherwise indicated. The desired thickness of the cured laminate was obtained by regulating the number of prepreg plies each of which contributed approximately 0.1 mm. The cured composite was scanned ultrasonically in order to detect flawed areas unsuitable for testing. Also,

photomicrographs of cross-sections parallel and perpendicular to the fiber axis were taken to examine the fiber distribution and alignment. The resin content was determined by acid digestion to be 22% by weight of the composite. The laminate was then precision cut into 30mm x 10mm samples at each of the following angles to the fiber direction:  $0^{\circ}$ ,  $15^{\circ}$ ,  $30^{\circ}$ ,  $45^{\circ}$ ,  $60^{\circ}$ ,  $75^{\circ}$ ,  $90^{\circ}$ .

#### Instrumental Measurements

The angle-cut samples and the neat resin were subjected to dynamic mechanical analysis on a commercial instrument which has been described in the literature (refs. 6 and 7). Each specimen was clamped at its ends between two parallel arms containing flexure pivots as depicted in Figure 1. One arm was driven at a low frequency while the other remained passive. The natural frequency of this sample support system was less than 3 Hertz (Hz). The imposed flexural stress induced a resonant frequency in the sample which was detected by a transducer. The oscillation amplitude of the driven arm was set at 0.20 millimeters peak-to-peak. The resonant frequency in Hz and relative logarithmic decrement in decibels (dB) were plotted on an x-y-y' recorder as a function of temperature. The heating rate was  $5^{\circ}\text{C}$  per minute.

Differential scanning calorimetry (DSC) and thermomechanical analysis (TMA) measurements were performed on commercial instruments. Standard experimental techniques were employed for both thermal methods. Samples were temperature scanned at a rate of  $20^{\circ}\text{C}/\text{minute}$ . Composite specimens were tested by TMA on the flat surface perpendicular to the fiber direction with a penetration probe. The sensitivity required to observe the thermal transitions corresponded to a probe displacement of 0.0001mm/mm of chart.

Sample temperature was monitored by a thermocouple placed inside the furnace directly adjacent to the sample. Thermomechanical and thermocouple responses were output to a two pen strip chart recorder.

### RESULTS AND DISCUSSION

The neat resin and composite glass transition temperatures were determined by DSC to be 78°C and 76°C, respectively, and were within experimental error ( $\pm 2^\circ$ ) of one another. The laminate was further characterized by photomicrography. Figure 2(a) is a cross-sectional view in which the fibers are perpendicular to the surface and shows small resin rich areas among randomly distributed fiber bundles. The alignment of the fibers is shown in Figure 2(b) in which the fibers are parallel to the surface. Most fibers appear to be nearly parallel and only a few are visibly misaligned.

Cured epoxy resins exhibit at least two damping peaks, one near -60°C and another in the glass transition region. The damping responses of the neat resin and laminate specimens in the low temperature region (the  $\beta$  transition) are generally attributed to the ether linkages of the molecule and were quite similar for all samples. In the glass or  $\alpha$  transition region, however, several differences were noted for the series of off-axis specimens. The most interesting observation was the appearance of an additional damping peak above the glass transition temperature of the matrix resin. Also, as the fiber direction was changed from transverse (90°) to longitudinal (0°), the  $\alpha$  transition region broadened and the change in frequency over this temperature range exhibited a maximum at intermediate angles.

For the 60° and 90° off-axis specimens cut from the 0.635mm thick laminate, it can be seen in Figure 3 that the shape of the damping curves remained almost as symmetric as that of the neat resin. For the 30° specimen the damping curve became skewed toward higher temperature (Figure 3).

As the angle was further decreased to  $15^{\circ}$ , a shoulder developed at a temperature above the  $\alpha$  transition. Figure 4 illustrates the growth of the shoulder into a peak of greater intensity than that of the resin  $T_g$  for low angle off-axis samples. It has been suggested that this type of behavior would be observed for an incompletely cured thermoset undergoing further cure during the dynamic mechanical test. This was clearly not the case in this study because all samples were cut from the same laminate and were subjected to the same thermal history. Furthermore, to insure that the additional damping peak was not due to stresses which are relieved by the first heating, as is often observed by DSC, each sample was cycled through the temperature range three times. Only slight changes occurred in the position of the damping peaks. In addition, a longitudinal sample was post-cured at  $204^{\circ}\text{C}$  for 4 hours to establish the effect of further curing. As is shown in Figure 5, the  $\alpha$  transition region was shifted to a higher temperature but the important point to note is that the two maxima in the damping curve remained.

Thicker laminates were also tested. Sample thickness was found to play a significant role in the observation of the new damping peak. The effect of increasing thickness was to diminish the peak until the curve became symmetric and resembled that of the high angle specimens as evidenced in Figure 6. Changes in the damping curves of specimens of identical composition but different thickness have been hypothesized to be due to unequal crosslink densities or to the specimen stiffness, which is directly proportional to the cube of the thickness, and obscures the higher temperature transition.

Other techniques were employed in an attempt to observe a thermal transition which may correspond to the new damping peak. The glass transition of the cured epoxy as well as the composite matrix resin were easily

discernible by both DSC and TMA. No other transition was observed by DSC, a not unexpected result since it is difficult to detect transitions more subtle than the glass transition in highly filled polymers. However, the TMA thermograms showed a change in slope above the resin  $T_g$  which corresponded to a change in the value of the thermal expansion coefficient. A representative TMA curve is reproduced in Figure 7. Although it cannot be unequivocally stated that the thermal transitions observed by TMA and DMA are related to one another, the results of the two methods are mutually supportive since the transitions found using each method occurred at approximately the same temperature as the other.

There are several possible explanations for the new damping peak. Although the damping in a composite is due primarily to the resin, the presence of a filler influences this behavior to the extent that new damping mechanisms can operate. This is especially the case when the filler material is chemically treated to increase resin adhesion, as in the silane sized glass fibers used in this work. The transverse glass/epoxy sample closely approximated the behavior of the neat resin, thus indicating that the molecular phenomena responsible for damping in the resin and in the composite probably were the same. However, as the fiber direction in the test specimen changed from  $90^\circ$  to  $0^\circ$ , the damping profile changed to include a second maximum above the  $\alpha$  transition of the epoxy resin for test specimens having angles less than  $30^\circ$ . The continued presence of the damping associated with the resin  $\alpha$  transition and the growth of another maximum at a higher temperature suggests that an additional mechanism is operative as the fiber orientation approaches the test direction.

It is generally accepted that there exists an interfacial region between resin and fiber in which the structure of the polymer is different



from that farther away, due to the attraction of the two phases for one another. The exact nature of this attraction is not known, but hypotheses including adsorption, chemical bonding and other interactions have been advanced. Neither is there much evidence pertaining to the interfacial region. Present speculations include:

A. A rigid polymer layer next to the filler surface with higher modulus caused by restricted end group motions (ref. 8).

B. A lower modulus polymer layer next to the surface resulting from residual thermal stresses (ref. 9).

C. A deformable resin layer adjacent to the surface which is different in composition from the bulk resin due to preferential adsorption (ref. 10).

This unique resin layer in the interface has been estimated to comprise roughly 0.1% of the total resin in a composite, assuming a thickness on the order of 100 Angstroms (ref. 8). It is reasonable to suppose that it would be most readily detectable when examining fiber-controlled composite properties, that is, when the interfacial layer is active in transferring the load to the fiber. The observed dynamic mechanical behavior of thin composite specimens lends support to the supposition. The transverse specimen whose properties were resin controlled behaved very much like the neat resin. The longitudinal specimen whose properties were fiber controlled retained the neat resin transition and exhibited a new damping peak not characteristic of the neat resin. It has been reported that it is possible for epoxies to exist as a matrix in which more highly crosslinked micro-gel particles are embedded (ref. 11). The damping curve of such a heterogeneous resin is broad and consists of two peaks compared to the narrow single peak of the homogeneous epoxy. The TMA results are consistent with a nonhomogeneous resin phase in the composite. The thermal expansion coefficient is sensitive to crosslink density, being higher for

less highly crosslinked samples. A change in slope of the TMA curve indicates a change in the coefficient of thermal expansion and two such changes occurred, one near the glass transition and the other 50° above the T<sub>g</sub>.

Other phenomena have been discovered to give rise to damping peaks above the glass transition. For example, acrylonitrile-butadiene-styrene polymers, designated ABS, have been shown to develop a new damping peak associated with molecular orientation induced by hot-stretching or cold-drawing (ref. 3). It was suggested that the orientation occurred in the interfacial region of the butadiene rubber and the acrylonitrile-styrene glass phases. The orientation and its associated damping peak were destroyed by annealing. For some partially crystalline and amorphous linear polymers a premelting damping peak is observed and is attributed to lattice or low molecular weight component motions. It is not likely that cross-linked networks such as epoxies could demonstrate orientation or premelting behaviors characteristic of linear chains, but it is almost certain that their structure in the immediate vicinity of a silane treated glass fiber would be different than that of the bulk resin. The interfacial polymer component would then have different chemical, thermal, and mechanical properties.

The change in shape of the damping curve with decreasing fiber orientation angle was accompanied by an increase in the width of the curve as well. The width of the transition was defined as the temperature range from the onset of damping to its return to the pre-transition level. The width remained approximately the same as that of the neat resin from 90° to 60°, after which it increased sharply as plotted in Figure 8, exhibiting the same behavior as the elastic modulus (ref. 12). Therefore, as the contribution of the fiber became larger, the  $\alpha$  transition relaxation was spread over a broader temperature range. It has been reported that the glass

transition width increases in a similar manner with increasing filler concentration in glass bead composites (ref. 1). The dependence of glass transition width on fiber orientation angle can also be interpreted as a concentration effect by implementing the concept of effective concentration. In this case the effective fiber concentration is that fraction of the total fiber present in the composite reflecting the extent of participation of the fiber at a given angle. Therefore, in a unidirectional laminate the effective concentration of fiber increases as the orientation angle decreases resulting in broader glass transition regions.

The change in resonant frequency through the glass transition was also found to be a function of fiber angle as shown in Figure 9. Unlike the glass transition width plot, the frequency change exhibited a maximum at approximately an angle of  $30^\circ$  as shown in Figure 10. Therefore, the specimens of intermediate angle sustained the largest loss in modulus through the glass transition.

The reinforcement of the fibers is evident both above  $T_g$  and below it and the change in frequency is a way of examining this effect. In the case of transverse specimens the fiber contribution is slight and properties are resin controlled both before and after  $T_g$ . For longitudinal specimens the fiber contribution is very significant and properties are fiber controlled both before and after  $T_g$ . However, for specimens of intermediate angles the resin was more effective at transferring the load to the fibers when in the glassy state than when in the rubbery state, and the frequency drop was larger than for the  $0^\circ$  and  $90^\circ$  samples. A function which behaves in a similar manner with respect to orientation angle is the longitudinal shear modulus (ref. 12). In this shear mode the resin in intermediate angle specimens transfers more load to the fibers than it does in the transverse or

longitudinal configurations. It is possible that the flexural strain imposed on the intermediate angle samples resulted in shear modes as well, thereby inducing the same functional form.

#### SUMMARY OF RESULTS AND CONCLUSIONS

The effect of fiber orientation on dynamic mechanical and thermal properties has been studied for unidirectional epoxy/glass laminates. A new thermal transition was observed in the composite material at a temperature above the glass transition temperature of the cured resin. The additional transition was revealed as a change in the thermal expansion coefficient as determined thermally and as a new damping peak as determined mechanically. Since this transition occurred in dynamic mechanical analysis only when the fiber direction was nearly parallel to the test direction, it was possibly a characteristic of the resin in the interfacial region, indicating a different resin structure adjacent to the glass surface.

The glass-rubber relaxation itself exhibited changes as the fiber direction was changed from transverse to longitudinal in the mechanical tests. As the fiber angle decreased from  $90^{\circ}$ , the temperature width of the glass transition was found to broaden, reflecting the increasing contribution of the fiber. Also, the change in resonant frequency through the glass transition was found to be a function of fiber angle exhibiting a maximum at intermediate angles. The width of the glass transition exhibited the same type of mathematical dependence on orientation angle as the elastic modulus; and the change in frequency displayed the same functional form as the longitudinal shear modulus.

## REFERENCES

1. D. H. Droste and A. T. DiBenedetto, "The Glass Transition Temperature of Filled Polymers and its Effect on Their Physical Properties," J. Appl. Polym. Sci., vol. 13, 1969, pp. 2149-2168.
2. T. Murayama, J. H. Dumbleton, and M. L. Williams, "The Viscoelastic Properties of Oriented Nylon 66 Fibers. Part III: Stress Relaxation and Dynamic Mechanical Properties," J. Macromol. Sci., vol. B1, no. 1, 1967, pp. 1-14.
3. J. H. Daane and S. Matsuoka, "Effects of Orientation on Dynamic Mechanical Properties of ABS," Polym. Eng. Sci., vol. 8, no. 4, 1968, pp. 246-251.
4. T. Murayama, J. H. Dumbleton, and M. L. Williams, "Viscoelasticity of Poly (ethylene Terephthalate)," J. Polym. Sci.: Part A-2, vol. 6, no. 4, 1968, pp. 787-793.
5. J. C. Seferis, R. L. McCullough, and R. J. Samuels, "Dynamic Mechanical Properties of Anisotropic Polypropylene Films," Appl. Polym. Symp. No. 27, 1975, pp. 205-228.
6. "Instruction Manual: Dynamic Mechanical Analyzer Model 980," DuPont Company, October 1976.
7. T. Murayama, Dynamic Mechanical Analysis of Polymeric Material, Elsevier Scientific Publishing Co., 1978, pp. 51-52.
8. R. L. McCullough, "Fundamental Concepts of Composite Materials," Document D1-82-09, Boeing Scientific Research Laboratories, Seattle, Wash., 1970, pp. 69-74.

9. L. E. Nielsen and T. B. Lewis, "Temperature Dependence of Relative Modulus in Filled Polymer Systems," J. Polym. Sci., Part A-2, vol. 7, no. 10, 1969, pp. 1705-1719.
10. P. W. Erickson, "Glass Fiber Surface Treatments: Theories and Navy Research," NOLTR 63-253, Naval Ordnance Lab., 1963.
11. L. E. Nielsen, "Cross-Linking - Effect on Physical Properties of Polymers," J. Macromol. Sci. - Rev. Macromol. Chem., vol. 3, no. 1, 1969, pp. 69-103.
12. L. E. Nielsen, Mechanical Properties of Polymers and Composites, Vol. 2, Marcel Dekker, Inc., 1974, p. 461.

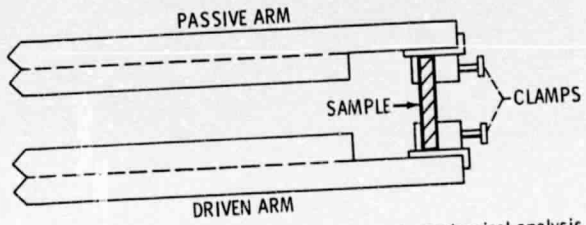
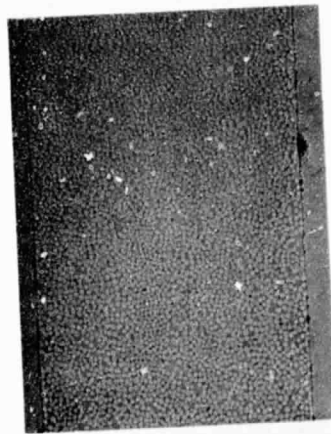


Figure 1. - Sample clamping geometry for dynamic mechanical analysis.



(a) PERPENDICULAR.



(b) PARALLEL TO FIBER DIRECTIONS.

Figure 2. - Photomicrographs of laminate cross sections.

ORIGINAL PAGE IS  
OF POOR QUALITY

E-631

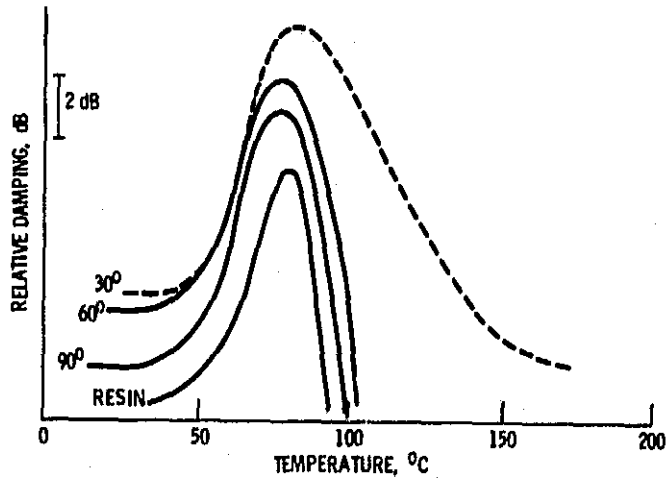


Figure 3. - Relative damping curves of 30°, 60°, 90° off-axis specimens and neat resin.

ORIGINAL PAGE IS  
OF POOR QUALITY

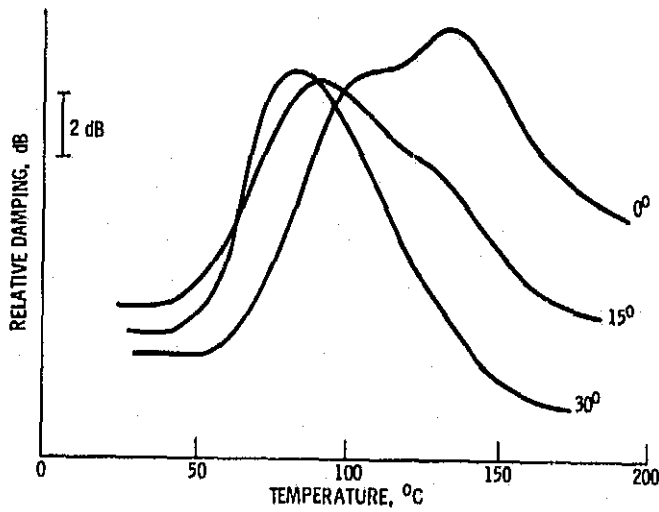


Figure 4. - Relative damping curves of 0°, 15°, 30° off-axis specimens.



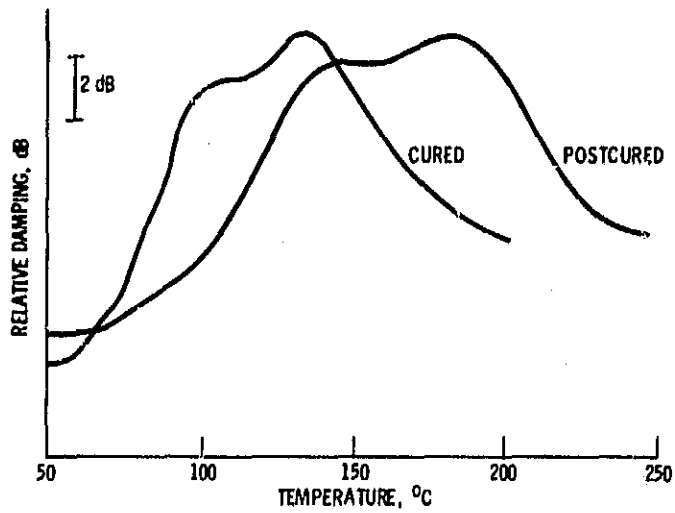


Figure 5. - Relative damping curves of cured and postcured longitudinal specimens.

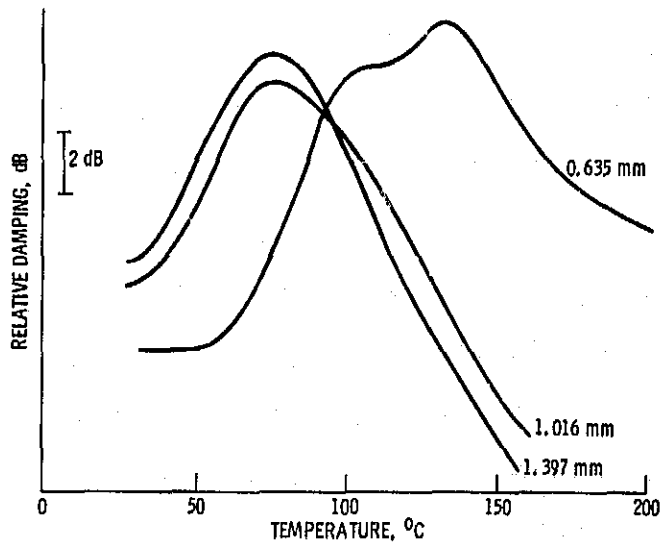


Figure 6. - Relative damping curves of 0.635 mm, 1.016 mm, and 1.397 mm thick longitudinal specimens.

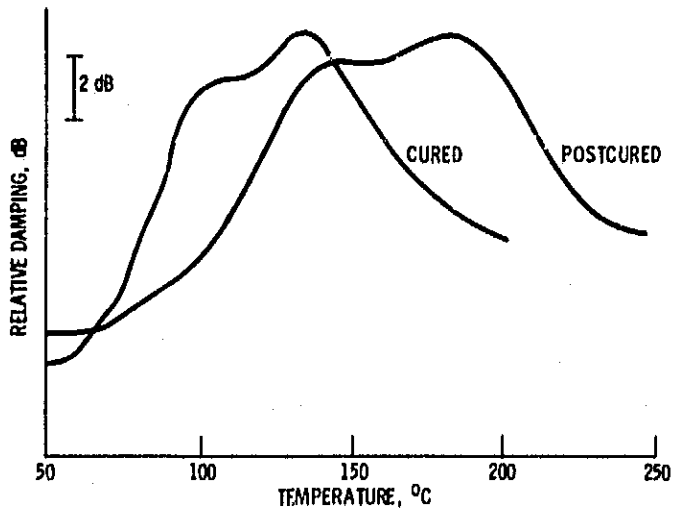


Figure 5. - Relative damping curves of cured and postcured longitudinal specimens.

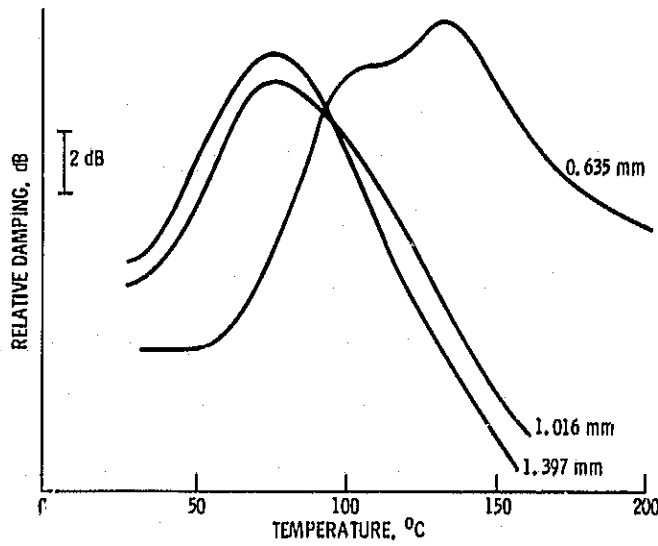


Figure 6. - Relative damping curves of 0.635 mm, 1.016 mm, and 1.397 mm thick longitudinal specimens.

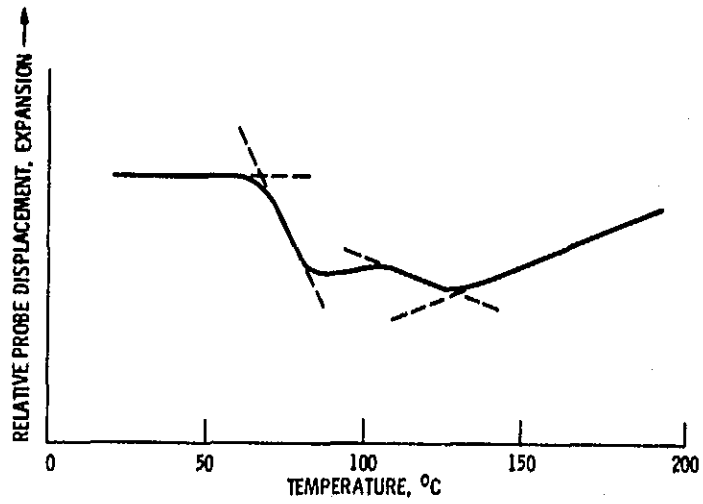


Figure 7. - Thermomechanical analysis curve of an epoxy/E glass unidirectional laminate.

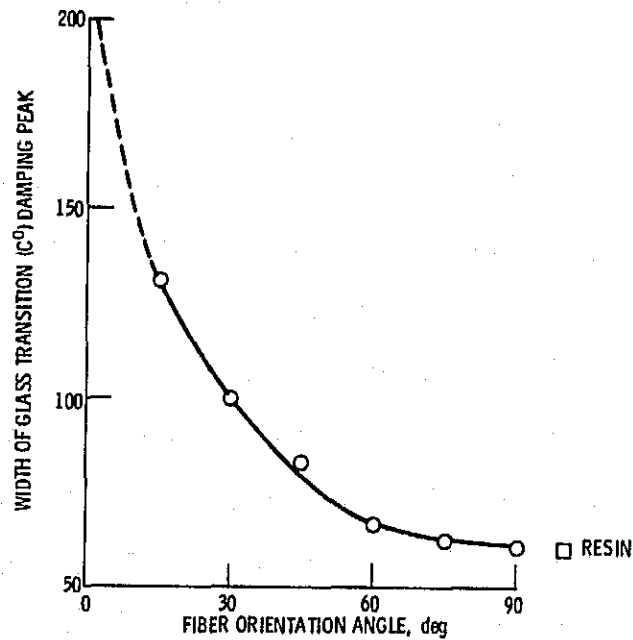


Figure 8. - Variation of glass transition damping peak width with fiber orientation angle.

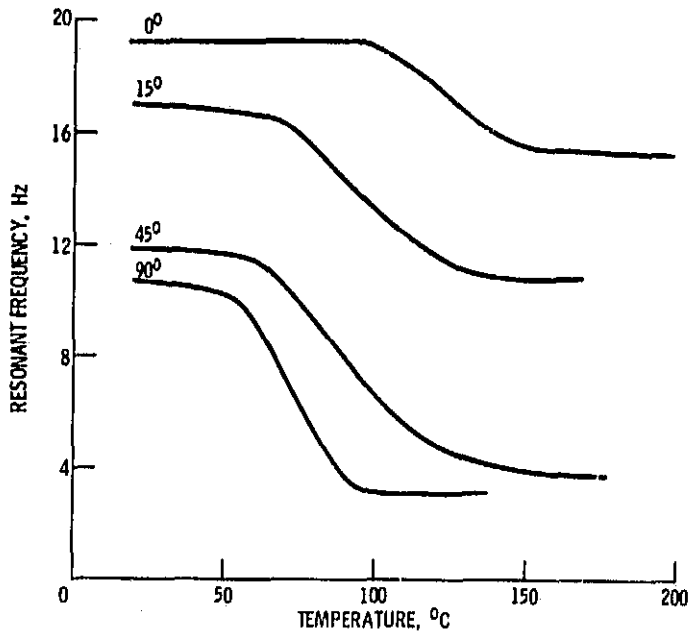


Figure 9. - Resonant frequency curves of 0°, 15°, 45°, 90° off-axis specimens.

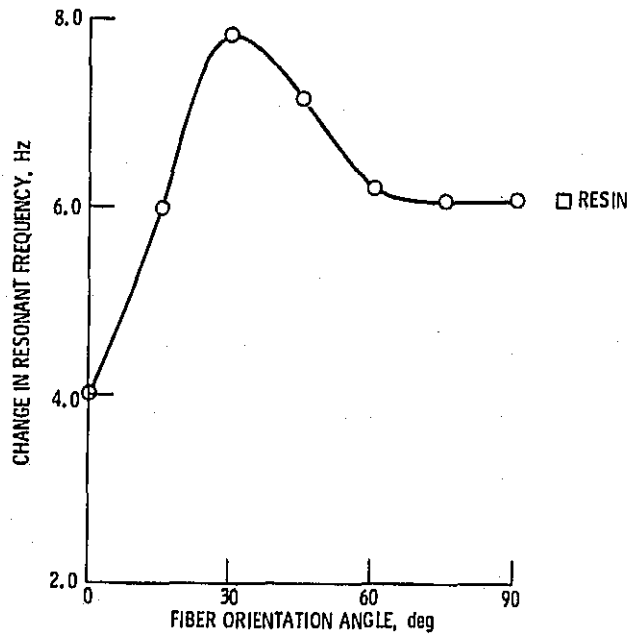


Figure 10. - Variation of resonant frequency drop with fiber orientation angle.